


## Article

# Experimental Study on Shield-Receiving Steel Sleeve Sealing Performance and Filler Pressure Regulation

Jiarui Qi <sup>1,2</sup>, Yiheng Pan <sup>1,2,\*</sup>  and Jinfeng Zhang <sup>3</sup><sup>1</sup> College of Harbour and Coastal Engineering, Jimei University, Xiamen 361021, China<sup>2</sup> Xiamen Key Laboratory of Green and Smart Coastal Engineering, Xiamen 361021, China<sup>3</sup> State Key Laboratory of Hydraulic Engineering Simulation and Safety, Tianjin University, Tianjin 300072, China

\* Correspondence: panyiheng@jmu.edu.cn

**Abstract:** Pressure balance control between steel sleeve fillings and stratum is the key to ensuring project safety in the receiving construction of subway shield tunnels. Here, to realize the active regulation of the filling pressure in the steel sleeve, this study first improves the fixed cover of a conventional steel sleeve to a piston cover that can slide freely along the longitudinal direction of the sleeve and puts forward the corresponding methods for hydraulic pressure regulation and mechanical pressure regulation. The pressure-holding sealing performance of a new steel sleeve structure was tested, and a hydraulic pressure regulation method and a mechanical pressure regulation method were proposed. Finally, an effective path to proactive filler pressure regulation in the steel sleeve was explored. By improving the structure scheme of the steel sleeve, A steel sleeve model was designed at a 1:5 proportion, following the shield receiving steel sleeve structures and their sizes in practical tunneling. The model test was performed for several processes of active control of filler pressure, including pressurization by injection, decompression by discharge, machinal pressurization in low pressure, machinal pressurization in high pressure, and machinal decompression. The laws of filler pressure variation with hydraulic pressure and machinal thrust, the reactive force of hydraulic jack, and stress of steel sleeve were researched. The results revealed that the maximum stress of the new steel sleeve structure was 14.5 MPa under an elastic stress state, and the circumferential stress was always eight times the longitudinal stress. The new steel sleeve structure shows controllable pressure-holding sealing performance. The hydraulic pressure decrease appears as a slow linear trend of about 0.1% of the initial pressure per min after 1 min of pressure holding. The variation in the filler pressure at the central position of the steel sleeve is 16–24% greater than that at the periphery. Both hydraulic pressure regulation and mechanical pressure regulation could achieve controllable proactive regulation effects on a steel sleeve's filler pressure. The proposed new shield-receiving steel sleeve structure and the study results about its sealing performance and filler pressure regulation will promote the shield-receiving technology to be more controllable and safer.



**Citation:** Qi, J.; Pan, Y.; Zhang, J. Experimental Study on Shield-Receiving Steel Sleeve Sealing Performance and Filler Pressure Regulation. *Appl. Sci.* **2023**, *13*, 7045. <https://doi.org/10.3390/app13127045>

Academic Editor: Tiago Miranda

Received: 8 April 2023

Revised: 8 June 2023

Accepted: 9 June 2023

Published: 12 June 2023

**Keywords:** shield tunnel; shield receiving; steel sleeve; pressure regulation

**Copyright:** © 2023 by the authors. Licensee MDPI, Basel, Switzerland. This article is an open access article distributed under the terms and conditions of the Creative Commons Attribution (CC BY) license (<https://creativecommons.org/licenses/by/4.0/>).

## 1. Introduction

The shield method has been widely used in urban metro tunnel construction due to its intelligent operation, fast tunneling speed, low labor intensity, and minor influence on road traffic [1–8]. During metro tunnel construction using the shield method, steps should be taken to address potential geohazards, including water ingress, stratum erosion, ground surface settlement, and tunnel face collapse [9–12]. Studies have suggested that there are high risks of water bursts and sand inrush during the shield tunneling receiving construction stage, which accounts for more than 50% of all accidents [13,14].

Recently, with the development of scientific research and engineering, some shield-receiving construction methods have been proposed and applied, including a physically

and chemically improved soil layers method, a novel material shield-cuttable tunnel-wall system construction method, an underwater receiving construction method, a steel sleeve receiving construction method, a concrete sealed cabin receiving construction method, a piston sealing steel ring receiving method and a receiving method in foamed concrete [15–21]. Steel sleeve receiving construction is a new method featuring space savings, safety, reliability and a minor influence on the environment. This method has been widely used in metro shield tunneling projects, including Guangzhou rail transit's Line 2, Line 8, and the Nanyan Line; the TA08 Fuqiao Station–Daxinggong Station section of Nanjing Metro Line 3; and the Nangang Station–Yonglu Station section of Guangzhou Metro Line 13 [22–24]. As a result, the steel sleeve-receiving construction method is useful for inhibiting surrounding ground settlement and building deformation, minimizing water leakage and sand inrush risks, accelerating construction speed and saving construction costs.

The conventional shield-receiving steel sleeve device is a circular bucket-like structure that is open at one end and sealed at the other (Figure 1). The open end connects the tunnel portal to form a closed container. Before the shield-receiving construction, the steel sleeve is filled with a mixture of sand and water; then, it is sealed after a certain pressure is reached and sustained [25]. The shield machine drives into the steel sleeve after tunnel excavation.

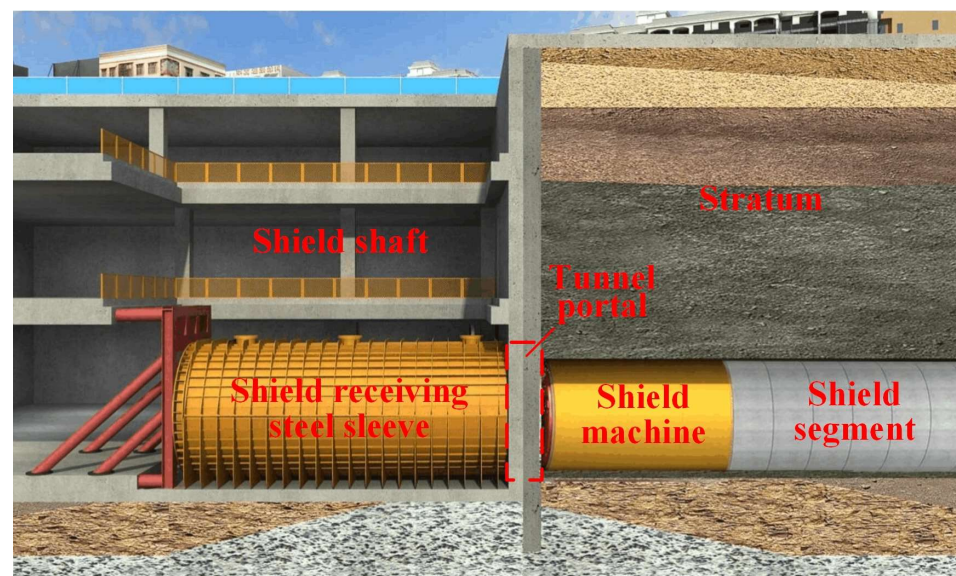


**Figure 1.** Receiving of shield machine by steel sleeve.

During the shield-receiving process, the inner space of the steel sleeve connects with the external stratum because the final shield segments were not installed. Construction safety is determined by the pressure balance between the steel sleeve's filler and the external stratum. When the pressure balance is mishandled, engineering risks, such as water bursts, sand inrush, and collapse, can more easily occur [26–28]. In conventional steel sleeve-receiving technology, the only part of the water and earth pressure in the stratum is passively balanced by filler pressure in the steel sleeve. During portal demolition, the soil and water of the stratum flow into the steel sleeve until complete pressure balance. Recently, studies on shield receiving with steel sleeves have focused mainly on project construction technologies and construction risks. Liu (2021) [29] studied the key technologies for steel sleeve-receiving of a large-diameter slurry shield in highly permeable silty-fine sand strata in coastal areas. Yang (2020) [30] and Zhou (2020) [31] analyzed the possible risk in steel sleeve receiving for metro shields and proposed a corresponding preventive measure to control construction risks. Liu et al. (2020) and Ji (2019) [32,33] introduced the detailed construction procedures of shield receiving by encapsulated steel sleeves and prefreezing. Wu et al. (2020) [34] studied the torsion resistance of steel sleeves in a case study of the Canapuri River tunnel in Bangladesh. Xu et al. (2019) [35] studied the combined scheme

of a cement system and vertical ground freezing for shield receiving and summarized the main construction parameters of the receiving stages. Liu et al. (2020) [36] introduced a combined technology of plain concrete diaphragm reinforcement and steel sleeves in shield-receiving construction, solving the problems of secondary reinforcement without working space. Wu (2017) [37] described the construction technology of a short sleeve for shield receiving to save construction costs. He (2015) [38] described a technical receiving technology of steel sleeves to solve the problem of hoisting steel sleeves without subsurface sites. However, studies on the stress-bearing and deformation laws of shield-receiving steel sleeves are rare. Liao (2016) [16] analyzed the rules of stress and deformation of steel sleeves by numerical methods and field tests. Zhou (2018) [39] studied the mechanical properties of steel sleeves and the soil disturbance patterns during the launching process through field monitoring tests and numerical simulations. However, few scholars have explored proactive control technology.

In this study, the conventional steel sleeve structure was improved. Specifically, the fixed cover plate of the original steel sleeve was first enhanced using a piston-type cover plate. Subsequently, two methods (i.e., the hydraulic and mechanical pressure regulation methods) that regulate the filler pressure in the sleeve were developed. The hydraulic pressure regulation method regulates filler pressure by setting an external hydraulic pressure regulation device on the sleeve body. The mechanical pressure regulation method applies a mechanical thruster onto the movable cover plate, which allows the surface pressure to act upon the internal filler to regulate filler pressure. To verify the feasibility of these two methods, various filler pressure regulation processes were tested, including pressurization by water injection, depressurization by water discharge, mechanical pressurization under low and high internal pressure levels, and mechanical depressurization. Finally, equations for the filler pressure in response to external hydraulic pressure, mechanical thrust and their action mechanisms were obtained, as well as the deformation equations of the steel sleeve body. This study aims to render a theoretical method to promote the engineering application of shield-receiving technology when the filler pressure is proactively controlled.

## 2. Test Profile

### 2.1. Specimen Design

A steel sleeve model was designed at a 1:5 proportion, following the shield-receiving steel sleeve structures and their sizes in practical tunneling (Figure 2). The steel sleeve model consists of two parts (i.e., a sleeve body and a cover plate), both of which were processed from Q235 steel (Table 1). The sleeve body was sealed at the lower end, with a height of 2.75 m and a thickness of 5 mm. The cover plate was 0.16 m in height and 1.18 m in outer diameter (Figure 3), allowing it to be horizontally inserted from the upper-end port of the sleeve body. Ribbed plates and pressure-bearing steel plates were arranged on the top of the cover plate, and a silica gel sealing ring covered the external lateral surface to seal the gap between the cover plate and the sleeve body. The results suggested that the sealing effect was best under a circumference of 3.7 m and a diameter of 12 mm.

**Table 1.** Measured steel material property indexes.

Yield Strength $f_s/\text{MPa}$	Tensile Strength $f_u/\text{MPa}$	Yield Strain $E_s/10^{-3}$	Elasticity Modulus $E_s/\text{MPa}$
292.8	418.0	1.44	$2.03 \times 10^5$



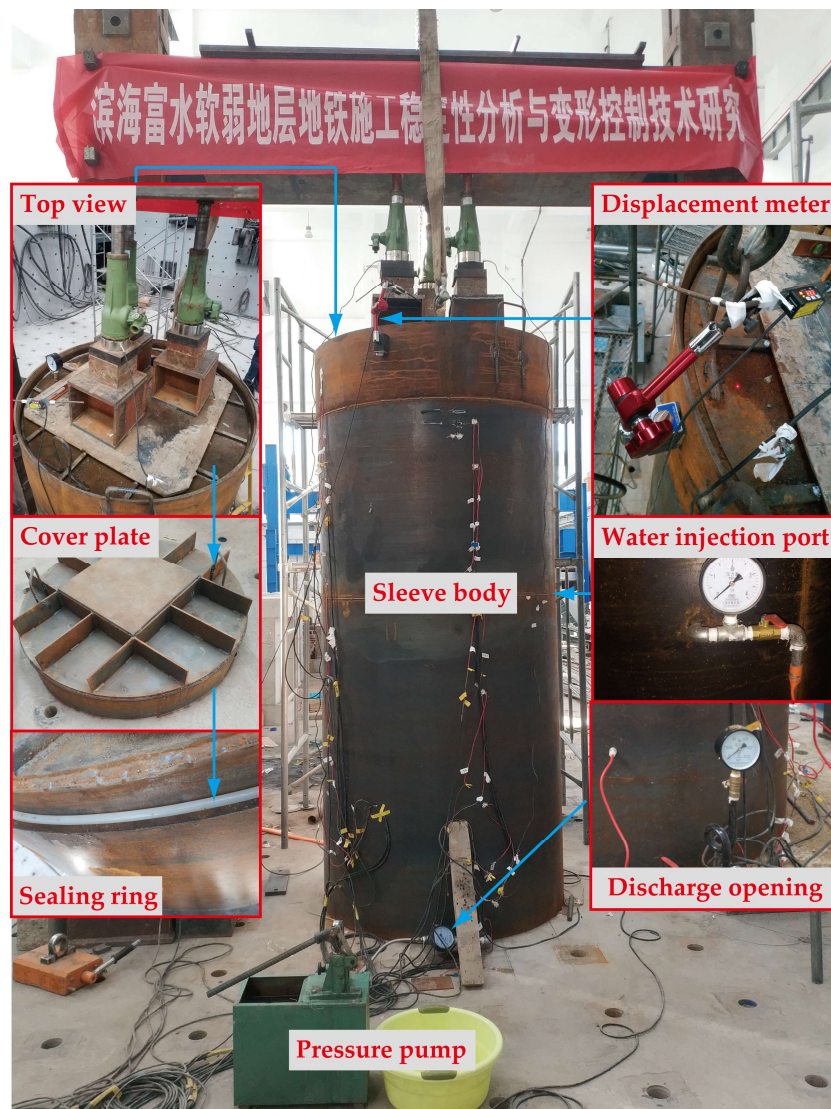


Figure 2. Test specimen and load-monitoring device.

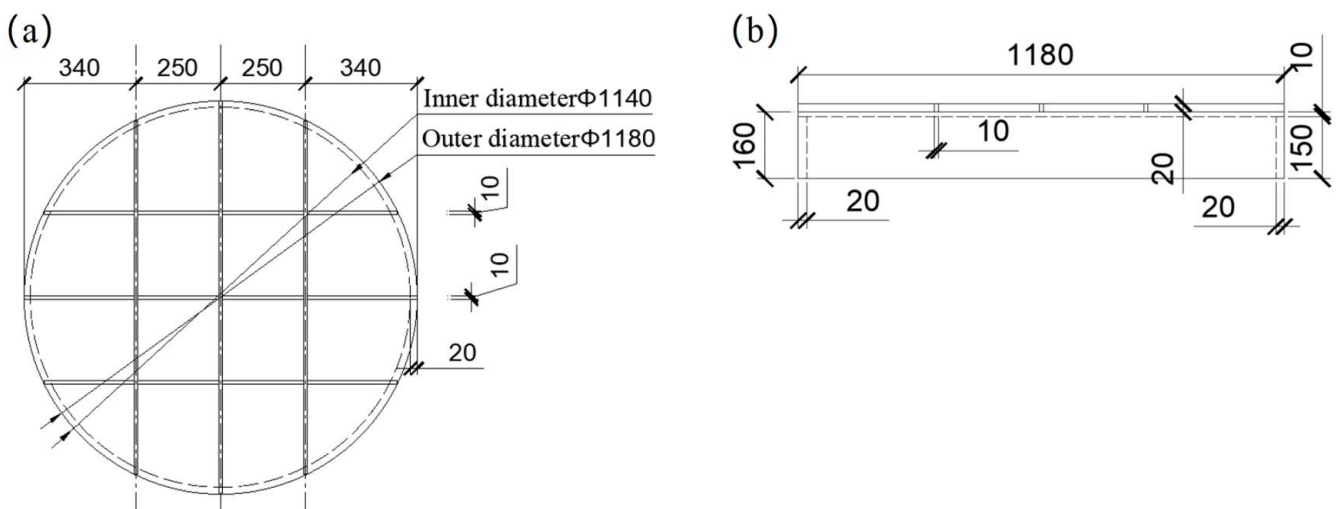


Figure 3. Design dimensions of the cover plate (mm). (a) Top view; (b) Side view.



### 2.2. Loading Test Scheme

The sealing performance of a steel sleeve under a certain internal pressure is the basis of the proactive control of internal filler pressure, and the pressure-holding sealing performance of this steel sleeve was implemented first. First, water was injected into the steel sleeve from the water injection port until the sleeve body was filled. Subsequently, the exhaust valve on the cover plate was closed for sealing. Next, water was injected into the sealed steel sleeve, and the internal water pressure was increased progressively in stages. During pressurization at each stage, the water injection valve was closed, followed by the pressure holding for 3 min. Pressurization was stopped when the internal water pressure exceeded 0.2 MPa and the pressure was held for 7 min. Finally, the valve was opened at the discharge opening (Figure 4). The ascent segment of the curve shows the pressurization test by water injection, the platform segment shows the pressure-holding test process, and the descent segment suggests the depressurization test process by water discharge.

To regulate the internal filler pressure, two methods (i.e., a hydraulic pressure regulation method and a mechanical pressure regulation method) were developed. Before the test, fillers were formed by mixing sand and water and were placed in the steel sleeve (Table 2). Next, the top face of the filler was leveled out using a level ruler, and the sleeve body was sealed after the hoisting cover plate was inserted into it. Subsequently, hydraulic pressure was regulated by water injection, while mechanical pressure regulation was realized by jack loading and unloading (Figure 2). In the water injection pressurization test, water was injected into the sleeve in stages (with the pressure increasing by 0.01 MPa in each stage). In the water discharge depressurization test, we opened the valve at the discharge opening to enable outward free water drainage. In the mechanical pressurization test under a low internal pressure level, the jack pressure was elevated in stages from 0 MPa. In the mechanical pressurization test under a high internal pressure level, the filler pressure inside was increased to a high level through water injection and held for several minutes to start the mechanical pressurization (Table 3).

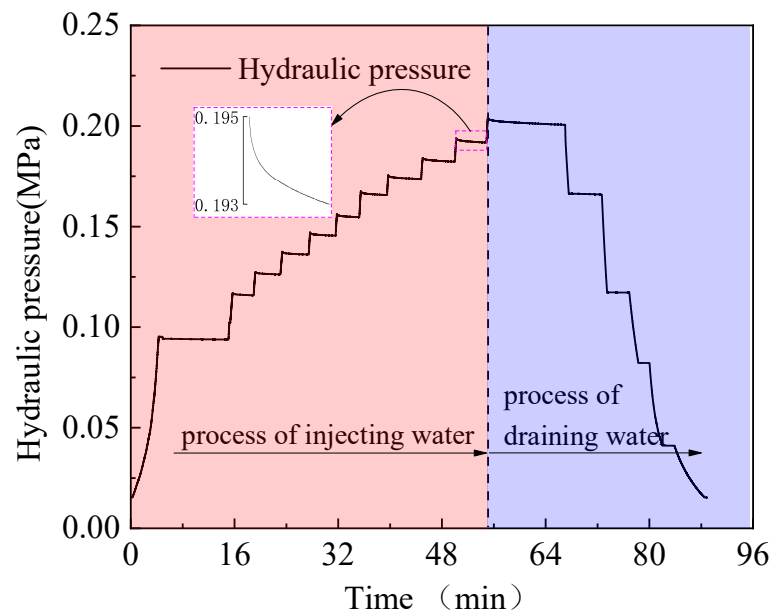


Figure 4. Internal water pressure time curve of the steel sleeve.

Table 2. Filler sieving test results.

Type	Cumulative Retained Percentage of Each Sieve Mesh/%						Fineness Modulus
	4.75	2.36	1.18	0.6	0.3	0.15	
Sand	1.90	19.24	35.78	53.12	80.17	90.41	2.97

**Table 3.** Loading test and load-monitoring scheme.

Loading Type	Loading Mode	Initial Load	Ending Load	Load Monitoring
Pressurization by water injection	Pressurization by pressure pump	0.02 MPa	0.16 MPa	Pressure at the water injection port
Depressurization by water discharge	Depressurization by water discharge	0.1 MPa	0.01 MPa	Pressure at the water discharge opening
Mechanical pressurization 1	Jack loading	0	116 kN	Reaction force of jacks
Mechanical pressurization 2	Jack loading	156 kN	199 kN	Reaction force of jacks
Mechanical depressurization	Jack unloading	199 kN	77 kN	Reaction force of jacks
Pressurization by water injection	Pressurization by pressure pump	0.02 MPa	0.16 MPa	Pressure at the water injection port

2.3. Layout of the Measuring Points

As shown in Figure 2, a total of four laser displacement meters were symmetrically arranged at the top of the cover plate to measure vertical displacement during the mechanical pressure regulation process. A pressure sensor was set between the jacks and the cover plate. A total of six strain-monitoring sections were arranged longitudinally along its surface (Figure 5). Along each monitoring section, two strain monitoring points (1 and 2) were arranged. At each point, one resistance-type strain gauge was placed along the horizontal and vertical directions to measure the circumferential and longitudinal strain on the steel sleeve body. Finally, a total of four vibrating wire-type earth pressure gauges were vertically buried inside the steel sleeve 0.4 m away from the bottom to measure the filler pressure changes within this plane. All data were obtained and recorded via a dynamic data acquisition system.

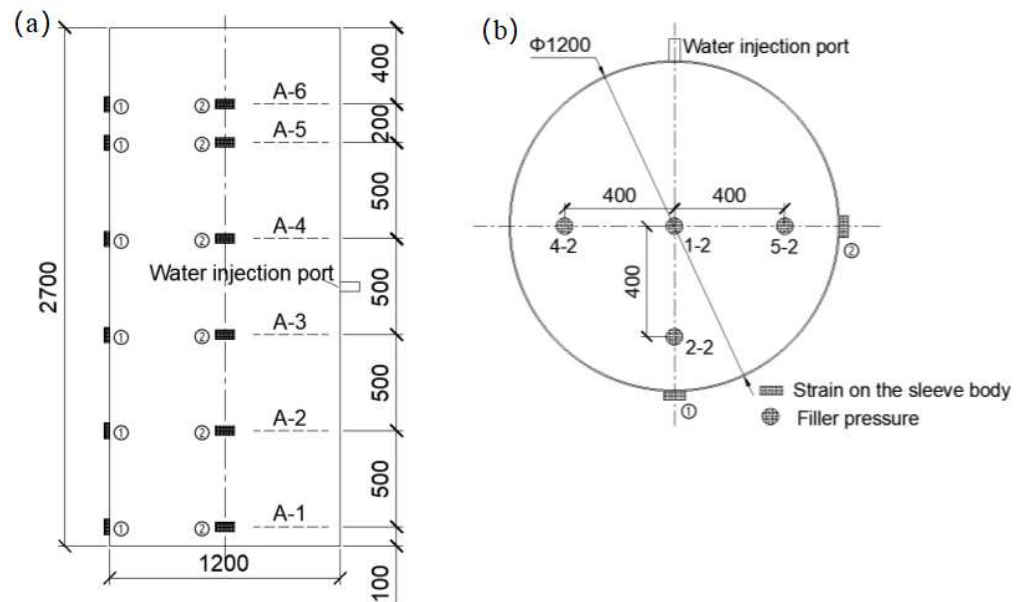


**Figure 5.** Measuring point layout plan (mm). (a) Longitudinal layout of the strain measuring points on the sleeve body; (b) Planar layout of the strain measuring points on the sleeve body and filler pressure.

### 3. Results and Discussion

#### 3.1. Steel Sleeve Pressure-Holding Sealing Performance

Figure 4 shows that the internal hydraulic pressure increases stably and rapidly during the whole pressurization process. Pressurization via water injection was initiated, the internal hydraulic pressure increased gradually, and the rate of increase gradually accelerated and stabilized at  $\sim 0.6$  KPa/s when the hydraulic pressure reached 0.075 MPa. The different rates of increase probably occurred because the cover plate slid slightly upward under hydraulic action and the jack at the top gradually pressed closer to the reaction force frame in the initial pressurization stage by water injection. In addition, the hydraulic pressure in the steel sleeve showed a slow declining trend in the pressure-holding test.

The internal pressure was generally lower than 0.2 MPa in the steel sleeve receiving process. Hence, the test data in the pressure-holding stage under different hydraulic pressures were selected for analysis. The steel sleeve hydraulic pressure loss time curves (Figure 6) were plotted to identify the hydraulic loss within 3 min. As a result, the hydraulic pressure in the steel sleeve was subjected to loss in the pressure-holding stage. The hydraulic pressure decreased rapidly within the first 10 s of pressure holding, accounting for  $\sim 40\%$  of the total hydraulic pressure loss. Subsequently, the hydraulic pressure loss rate quickly decreased and stabilized at approximately 1 min, while the internal hydraulic pressure continuously decreased. The greater initial hydraulic pressure resulted in a higher hydraulic pressure loss rate, while the absolute hydraulic pressure loss under each initial pressure level was always lower than the corresponding magnitude of the pressure value.

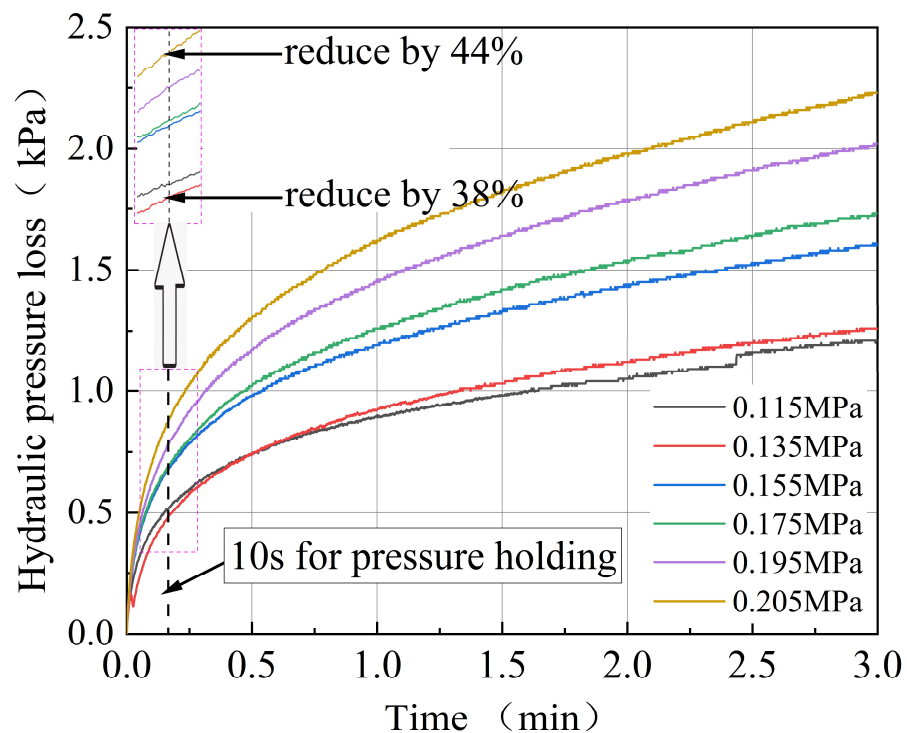


**Figure 6.** Steel sleeve hydraulic pressure loss time curves (pressure holding time: 3 min).

The hydraulic pressure loss curve inside the steel sleeve within 12 min under an initial hydraulic pressure of 0.205 MPa is shown in Figure 7. As a result, after 3 min of pressure holding, the hydraulic pressure loss shows a linear growth trend, and the pressure loss rate was approximately 0.16 KPa per min, which accounted for only 0.08% of the initial pressure. Therefore, the filler pressure loss inside was stable and sustained at a low speed, and it could be naturally eliminated with normal filler pressure regulation during shield receiving. This would generate no adverse effects on the internal filler pressure regulation.



Figure 8 shows the relationships between the internal hydraulic pressure and the stress on the steel sleeve body in the pressurization stage. The results show that the circumferential stress was always eight times the longitudinal stress. Except for the A-1 monitoring section at the bottom, the longitudinal stress was similar to the circumferential stress at other positions. Moreover, the pressure in section A-1 was much smaller than that in the other sections, which was probably because the internal pressure induced by the hydraulic pressure at this position was borne by the nearby sealing steel plate at the bottom. During the test, when the hydraulic pressure in the steel sleeve reached its maximum value (0.205 MPa), the maximum tensile stress and maximum compressive stress were 14.5 MPa and 2.5 MPa, respectively. The maximum stress is only 6% of yield strength suggesting a low elastic stress level. The design of the shield-receiving steel sleeve in practical tunneling is conservative, and the thickness of the steel sleeve body should be decreased according to the test result of stress and expectant safety.

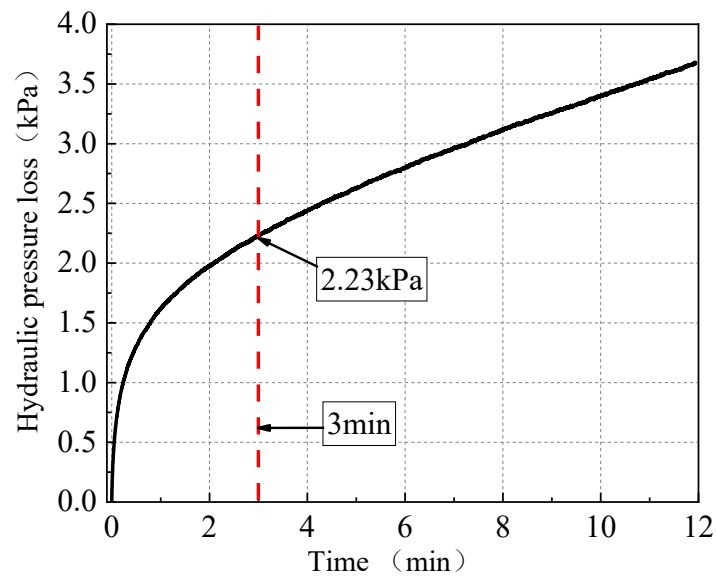


Figure 7. Steel sleeve hydraulic pressure loss time curve (pressure holding time: 12 min).

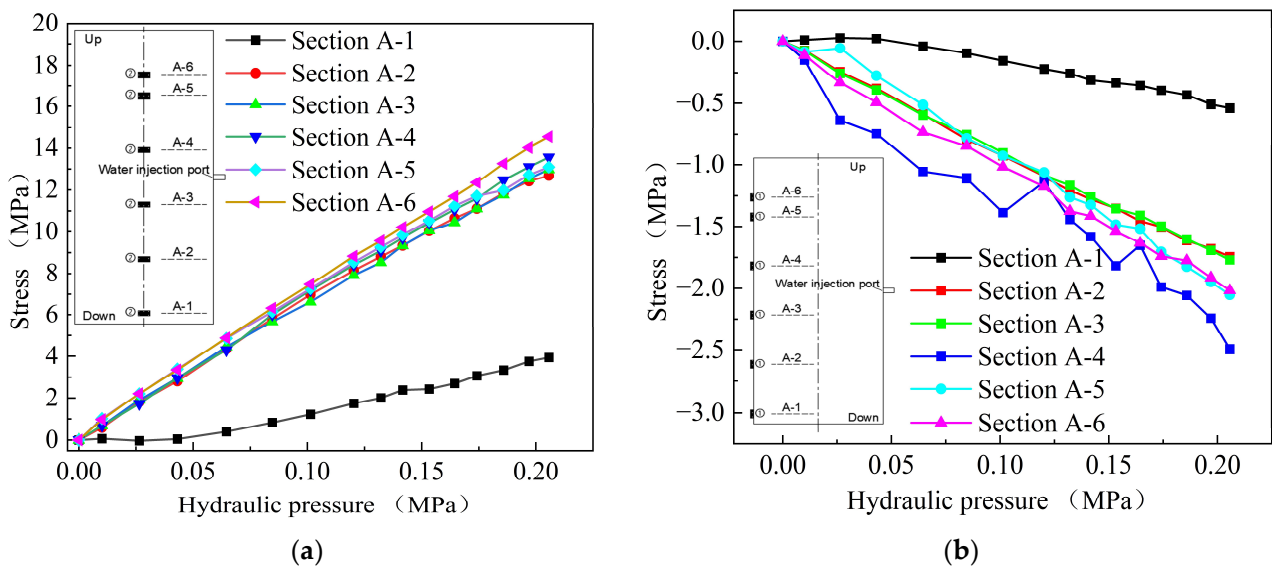
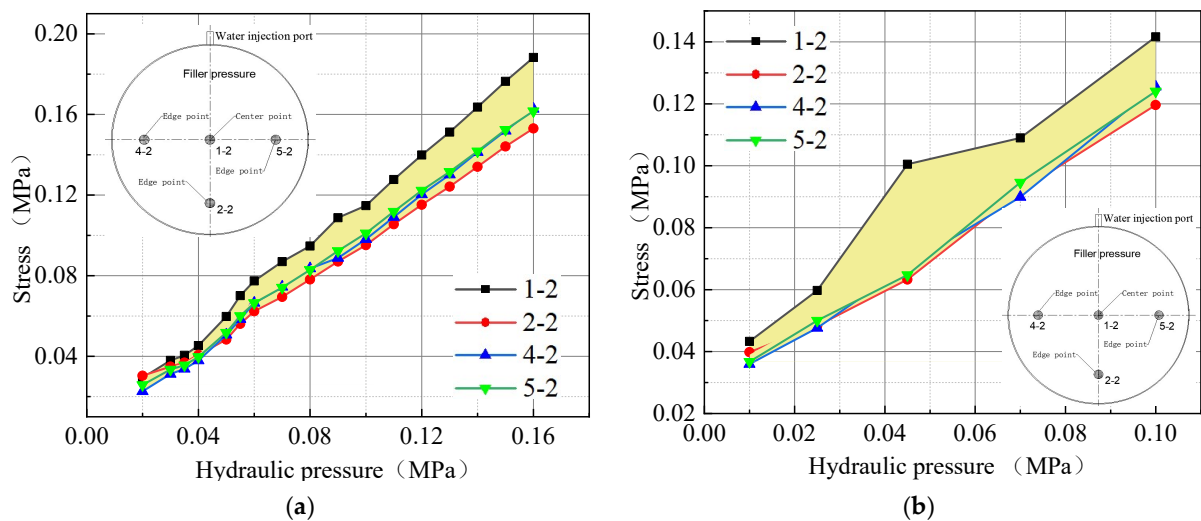


Figure 8. Hydraulic pressure stress on the sleeve body curves. (a) Circumferential stress; (b) Longitudinal stress.

### 3.2. Results and Analysis of the Hydraulic Pressure Regulation Test

As shown in Figure 9a, when the water injection pressure increased gradually from 0 to 0.16 MPa, the filler pressure at each measuring point showed a linear growth trend before reaching 0.15–0.18 MPa. The filler pressure was almost identical at all measuring points when the water injection pressure was lower than 0.04 MPa. As the water injection pressure continued to increase, the filler pressure at two peripheral measuring points (4-2 and 5-2) was consistent, while it increased quickly at the central point (1-2) and increased slowly at the peripheral measuring point (2-2). With a water injection pressure of 0.16 MPa, the filler pressure at the measuring points of the two peripheral sides was 14% lower than that at the central measuring point and 6% higher than that at the distant measuring points. When the water injection pressure varied within the range of 0.04–0.16 MPa, the difference in pressure between different measuring points could be estimated based on the linear difference value. The reason for the pressure difference in different positions of filler is the various seepage path. The mean value of filler pressure results in measuring points can be calculated as the normal reference values of filler pressure.



**Figure 9.** Hydraulic pressure-filler pressure curves. (a) Pressurization by water injection; (b) Depressurization by water discharge.

The filler pressure at each measuring point along each filler pressure monitoring section decreased linearly with the decline in pressure at the water discharge opening from 0.1 to 0.01 MPa (Figure 9b). The curves of the measuring points at these two peripheral sides (4-2 and 5-2) overlapped with the distant peripheral measuring point (2-2). The filler pressure at the central measuring point (1-2) declined at a high decreasing rate, but its pressure difference from other measuring points gradually narrowed with depressurization until the difference was negligible. The results in Figure 9 show that when the water injection port was pressurized by one bar or when the water discharge opening was depressurized by one bar, the mean value of the filler pressure on each monitoring section increased or decreased by one bar.

### 3.3. Results and Analysis of the Mechanical Pressure Regulation Test

As shown in Figure 10, the filler pressure increased with mechanical pressurization under a low internal pressure level (less than 0.15 MPa), which could be divided into three stages. When the jack pressure was lower than 40 kN, the filler pressure increased slowly. However, it increased quickly for jack pressures in the range of 40 to 45 kN. Finally, the filler pressure increased stably with the jack pressure at a gradually decreasing growth rate. During the whole pressurization process, the filler pressure at all measuring points followed change curves. The filler pressure at the peripheral measuring points overlapped the change curves, whereas it grew faster at the central measuring point.

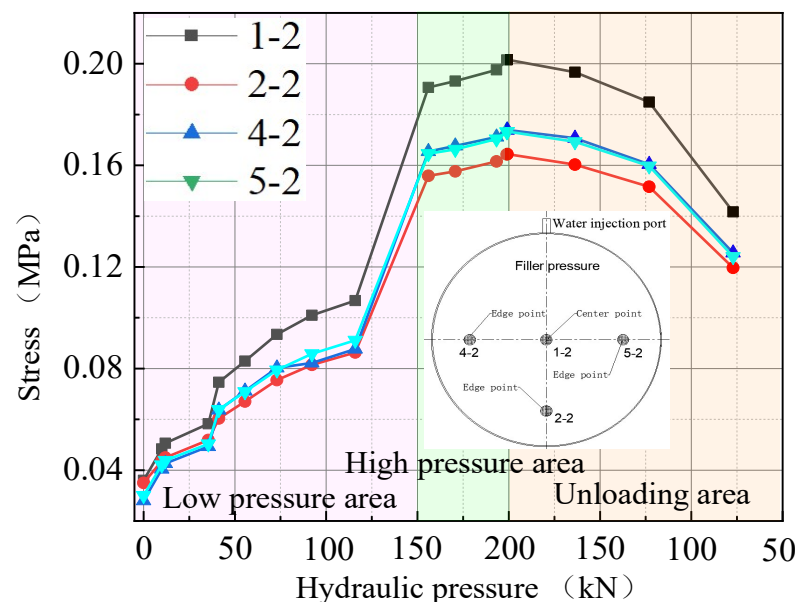


Figure 10. Jack pressure-filler pressure curves.

A pressurization test under a high internal pressure level was conducted when the filler pressure reached a high level (greater than 0.15 MPa) (Figure 10). In this case, the difference between the initial value of the filler pressure at the central measuring point (1-2) and that at the peripheral measuring points (2-2, 4-2, and 5-2) was further increased. The filler pressure at the measuring points of the two peripheral sides (4-2 and 5-2) was different from that at the peripheral distant measuring point (2-2). During the test, the filler pressure at each measuring point showed a linear growth relationship as the jack pressure increased continuously from the initial pressure of 150 kN. When the jack pressure increased by 1 kN, the filler pressure at the peripheral measuring point increased by 0.2 MPa, and that at the central measuring point increased by 0.25 KPa.

As shown in the unloading area of Figure 10, the filler pressure at each measuring point declined with the reduction in jack pressure, and the deceleration rate was inversely proportional to the jack pressure. The filler pressure at the central measuring point declined the fastest, followed by those at the two peripheral sides and the peripheral distant measuring point. Thus, the filler pressure difference between different measuring points was gradually narrowed during the depressurization process.

Compared with the hydraulic pressure regulation process, the mechanical pressure regulation process was more complicated, especially the mechanical pressurization method using a low internal pressure level. During the mechanical pressure regulation, a proactive pressure was applied to the filler inside the steel sleeve by multiple jacks, but the filler was an inhomogeneous semifluid mixture composed of sandy soil, water, and air. Under a low jack pressure, the filler was relatively loose and nonuniform, and the compressive deformations at the points of action of different jacks differed considerably. As a result, the cover plate was more prone to tilt and further contacted the inner wall of the steel sleeve. In this case, the partial jack pressure was directly transferred to the steel sleeve and effectively transferred to the filler. Thus, the filler pressure grew slowly during the test when the jack pressure was lower than 40 kN. Subsequently, as the jack pressure was increased, the pressure and displacement of each jack were dynamically adjusted, the deviation of the cover plate was corrected, and the partial pressure directly acting upon the sleeve was redistributed to the filler, which resulted in a sudden increase in filler pressure. The filler was gradually compacted after compression, exhibiting more stable and homogeneous mechanical properties, which facilitated the stable control of the pressure and displacement of each jack. Finally, the cover plate steadily applied pressure inside the sleeve, and the filler pressure stably changed with the jack pressure.



Under a low internal pressure level, the filler pressure was elevated with mechanical pressurization, which was manifested in three stages (Figure 10). The filler pressure changed stably during mechanical pressurization and depressurization under a high internal pressure level. The variation trend of the displacement of the cover plate with the jack pressure was consistent with the filler pressure under each working condition (Figure 11), and their features can be explained by the aforementioned changes in the filler pressure. During the practical engineering of the mechanical pressurization process, when the filler pressure did not increase stably with the jack pressure, the cover plate deviated excessively, as evidenced by the displacement monitoring result of the cover plate.

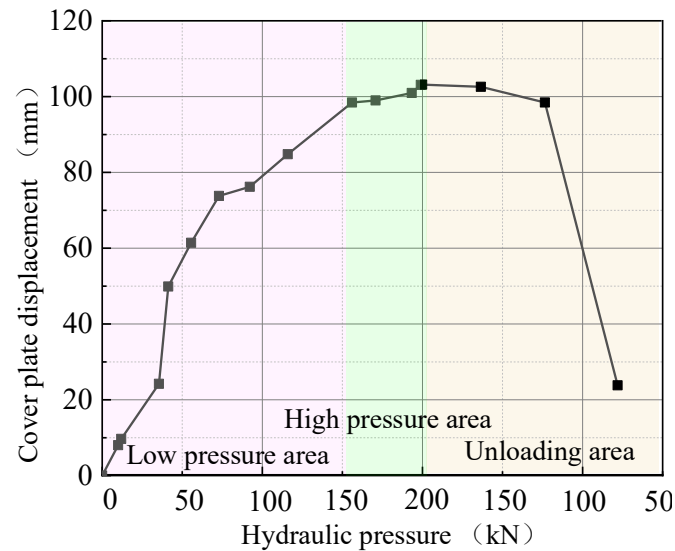


Figure 11. Jack pressure-cover plate displacement curves.

#### 4. Conclusions

Both hydraulic pressure regulation and mechanical pressure regulation could achieve controllable proactive regulation effects on a steel sleeve's filler pressure. The detailed conclusion includes five parts as follows.

- (1) By hydraulic pressure regulation, the linear and equally proportional variation in the filler pressure of the steel sleeve in response to external hydraulic pressure variation is observed. The pressure variation at the entrance point of the filler pressure monitoring cross section is 16~24% larger than that at the peripheral measuring points.
- (2) During mechanical pressure regulation, the pattern of its increase and decrease is obvious, the action mechanism is clear, and the pressure value is steady and controllable. Under the low internal pressure level (less than 0.15 MPa), the nonlinear variation in filler pressure is complicated by mechanical pressurization which could be divided into three stages. The filler pressure changed stably during mechanical pressurization and depressurization under a high internal pressure level (greater than 0.15 MPa).
- (3) The maximum stress of the new steel sleeve structure was 14.5 MPa under an elastic stress level. Variations in the jack reaction forces and cover plate displacement are stable, guaranteeing the safety of the steel sleeve structure.
- (4) Under the low internal pressure level (greater than 0.15 MPa), the operation of mechanical pressure regulation requires more prudential control. The slight slant of the cover plate should be dynamically revised by accurate adjustment of Jack pressure, and normal mechanical pressure regulation should implement after pressurization to 0.05 MPa via water injection. A simple and stable method involves regulating filler pressure using the hydraulic pressure regulation method. However, with the use of the mechanical pressure regulation method, faster regulation effects will be obtained with higher control precision. Two methods for regulating filler pressure should be selected according to practical operational capacity and pressure regulation requirements.

- (5) Under the proposed design scheme, the pressure in the steel sleeve is still slowly lost during pressure holding, and absolute sealing cannot be achieved in the whole pressure regulation process. The present solution is to compensate for the pressure according to the pressure monitoring result. The design scheme should be optimized from the view of seal ring material and seal structure design, and further related research work will be carried out. In addition, the current research is only on the principle and performance of the filler pressure regulation for the new steel sleeve structure, and the specific construction technology needs to be further studied in the engineering application.

**Author Contributions:** Conceptualization, J.Q. and Y.P.; Methodology, J.Q. and J.Z.; Validation, Y.P.; Writing—original draft preparation, J.Q. and Y.P.; Writing—review and editing, J.Z.; Funding acquisition, J.Z. All authors have read and agreed to the published version of the manuscript.

**Funding:** This study was funded by the National Key Research and Development Program of China (Grant No. 2021YFB2601100), the National Natural Science Foundation of China (Grant No. 52109087), the Natural Science Foundation of Fujian (Grant No. 2020J05145), and the Science and Technology R&D Program of China Construction Infrastructure Co., Ltd. (Grant No. CSCIC-2021-KT-02). The authors gratefully appreciate the support provided.

**Institutional Review Board Statement:** Not applicable.

**Informed Consent Statement:** Not applicable.

**Data Availability Statement:** The data presented in this study are available upon request from the corresponding author.

**Acknowledgments:** The authors would like to acknowledge the administrative and technical support given by Jie Yuan and Chen Ye.

**Conflicts of Interest:** The authors declare no conflict of interest.

## References

1. Youn, B.Y.; Breitenbücher, R. Influencing parameters of the grout mix on the properties of annular gap grouts in mechanized tunneling. *Tunn. Undergr. Space Technol.* **2014**, *43*, 290–299. [[CrossRef](#)]
2. Li, X.G.; Yuan, D.J. Response of a double-decked metro tunnel to shield driving of twin closely under-crossing tunnels. *Tunn. Undergr. Space Technol.* **2012**, *28*, 18–30. [[CrossRef](#)]
3. Qian, F.; Du, J.M.; Wang, Z.J.; Liu, X. Model experimental study on stratum deformation of shield tunnelling in sand. *China J. Highw. Transp.* **2021**, *34*, 135.
4. Cheng, H.Z.; Chen, J.; Chen, G.L. Analysis of ground surface settlement induced by a large EPB shield tunnelling: A case study in Beijing, China. *Environ. Earth Sci.* **2019**, *78*, 605. [[CrossRef](#)]
5. Zhu, C.; Li, N. Prediction and Analysis of Surface Settlement Due to Shield Tunneling for Xi'an Metro. *Can. Geotech. J.* **2017**, *54*, 529–546. [[CrossRef](#)]
6. He, X.C.; Xu, Y.S.; Shen, S.L.; Zhou, A.N. Geological Environment Problems during Metro Shield Tunnelling in Shenzhen, China. *Arab. J. Geosci.* **2020**, *13*, 87. [[CrossRef](#)]
7. Liu, W.Z.; Sun, K.; Dai, X.Y.; Ai, G.P.; Lei, T. Numerical Simulation and Field Monitoring of Influence of Metro Shield Tunnel Undercrossing the Existing Railway Frame Bridge by Long Distance. *J. Railw. Sci. Eng.* **2022**, *19*, 208–218.
8. Lin, R.A.; Sun, Y.F.; Dai, Z.H.; Weng, X.L.; Wu, Y.H.; Luo, W. Predicting for Ground Surface Settlement Induced by Shield Tunneling in Upper-soft and Lower-hard Ground Based on RS-SVR. *China J. Highw. Transp.* **2018**, *31*, 130–137.
9. Liu, X.X.; Xu, Y.S.; Cheng, W.C. Investigation of Hydraulic Parameters of a Weathered Mylonite Fault from Field Pumping Tests: A case study. *Bull. Eng. Geol. Environ.* **2017**, *76*, 1431–1448. [[CrossRef](#)]
10. Ren, D.J.; Shen, S.L.; Cheng, W.C. Geological Formation and Geo-Hazards during Subway Construction in Guangzhou. *Environ. Earth Sci.* **2016**, *75*, 934. [[CrossRef](#)]
11. Fang, Y.; Chen, Z.; Tao, L. Model Tests on Longitudinal Surface Settlement Caused by Shield Tunnelling in Sandy Soil. *Sustain. Cities Soc.* **2019**, *47*, 101504. [[CrossRef](#)]
12. Zhang, Z.X.; Liu, C.; Huang, X. Numerical Analysis of Volume Loss Caused by Tunnel Face Instability in Soft Soils. *Environ. Earth Sci.* **2017**, *76*, 563. [[CrossRef](#)]
13. Hu, Q.F.; Qin, J.B. Statistical Analysis on Accidents of Subway Tunnel Construction from 2003 to 2011 in China. *Chin. J. Undergr. Space Eng.* **2013**, *9*, 705–710.
14. Li, F.W.; Du, X.L.; Zhang, M.J. Statistical Analysis of Accidents in Metro Construction. *Chin. J. Undergr. Space Eng.* **2014**, *10*, 474–479.

15. Ben, Z.J.; Yang, P.; Chen, C.J.; Wang, S.F. Water Receiving Technology of Large Slurry Shield in River-crossing Subway Tunnel. *J. Nanjing For. Univ. (Nat. Sci. Ed.)* **2015**, *39*, 119–124.
16. Liao, S.M.; Men, Y.Q.; Zhao, G.Q.; Xu, W.Z. Mechanical Behaviors and Field Tests of Steel Sleeves During Shield Receiving. *Chin. J. Geotech. Eng.* **2016**, *38*, 1948–1956.
17. Sun, T.S.; Chen, S.M. New Technology of Large-diameter Shield Excavation on Tunnel Portal. *Urban Mass Transit* **2012**, *15*, 95–98.
18. Zhou, C.; Yu, Q.Z.; Yang, J. Risk Control Technology of Leakage Accident for the Subway Arriving. *J. Railw. Eng. Soc.* **2016**, *33*, 99–104.
19. Wang, S.J.; Zhang, J.P. Shield-Driven Initiation Technology of Reinforced Concrete Sealed Cabin in the Concealed Working Well of Metro Engineering. *Urban Mass Transit* **2020**, *23*, 165–168.
20. Chang, X. Piston Sealing Steel Ring Receiving Technology of Slurry Shield. *Constr. Technol.* **2017**, *46*, 106–108.
21. Liu, M.B.; Liao, S.M.; Chen, L.S.; Zhao, G.Q.; Xu, W.Z. In-Situ Measurements of Shield Machine Receiving in Foamed Concrete. *Chin. J. Geotech. Eng.* **2020**, *42*, 2006–2014.
22. Zheng, S.; Ju, S.J. Technology of Steel Reception Sleeve for Slurry Shield. *Mod. Tunn. Technol.* **2010**, *47*, 51–56.
23. Zhao, L.F. Auxiliary Construction Technology with Steel Sleeve Used for the Arrival of Soil Pressure Balance Shield. *Railw. Stand. Des.* **2013**, *8*, 89–93.
24. Wu, W.L.; Wang, H.J.; Gao, K.; Zou, Y. Application of Steel Sleeve Balance Technology in Slurry Balance Shield Tunneling. *Urban Mass Transit* **2016**, *19*, 125–128.
25. Zhu, H.Y.; Jia, L.; Feng, H.H. Steel Sleeve Receiving Technology for Shield Construction in Zhengzhou Rail Transit Line 2. *Constr. Technol.* **2016**, *45*, 122–127+140.
26. Wang, T.M.; Dai, Z.R. Application on Ground Reinforcement Method of Launching Shaft for Shield Tunnel. *J. Railw. Eng. Soc.* **2014**, *31*, 90–95+100.
27. Zhao, J.; Dai, H.J. Shield Break-in and Break-out Techniques in Soft Soil for Shield Driven Tunnel. *Chin. J. Rock Mech. Eng.* **2004**, *52*, 5147–5152.
28. Sun, Y.; Liu, M.G.; Lu, P.; Chen, R.D.; Pang, K. Review of Key Technical Issues in Construction of Cross Passage in Shield Tunnel. *Mod. Tunn. Technol.* **2021**, *58*, 293–302.
29. Liu, H.; He, Y.; Zhong, H.; Zhang, F.L. Key Technologies for Steel Sleeve Receiving of a Large-Diameter Slurry Shield in Water-Rich Silty-Fine Sand Strata in Coastal Area: A Case Study of Karnaphuli River-Crossing Tunnel in Bangladesh. *Tunn. Constr.* **2021**, *41*, 1225–1233.
30. Yang, S.B. Risk Analysis and Preventive Measures of Metro Shield Steel Sleeve Receiving. *Eng. Technol. Res.* **2020**, *5*, 180–181.
31. Zhou, L. Study on Risk Evaluation and Countermeasures of Metro Shield Steel Sleeve Receiving Construction. Ph.D. Thesis, Lanzhou Jiaotong University, Lanzhou, China, 2020.
32. Liu, Y.J.; Yang, Z.L.; Yang, T.; Yin, Q.F.; Chen, L.; Gu, X.F. Shield Receiving Technology by Encapsulated Steel Sleeve and Pre-freezing. *Mod. Tunn. Technol.* **2020**, *57*, 974–979.
33. Ji, W.J. Application of Freezing Combined Steel Sleeve Construction Technique to Shield Receiving in Metro Tunnel. *Mod. Tunn. Technol.* **2019**, *56*, 660–664.
34. Wu, Z.S.; He, Z.H.; Liu, W.; Xu, C.; Kong, Q. Torsion-resistant Construction Technology for Steel Sleeve Used in Launching of Large-diameter Slurry Shield: A Case Study of Canapuri River Tunnel in Bangladesh. *Tunn. Constr.* **2020**, *40*, 321–326.
35. Xu, J.B.; Wang, F.; Fu, C.; Song, W. Combined Application of Cement System and Vertical Ground Freezing to Shield Receiving in Wuhan Metro Tunnel Construction. *Tunn. Constr.* **2019**, *39*, 358–365.
36. Liu, Y.J.; Yang, Z.L.; Yang, T.; Yin, Q.F.; Chen, L.; Gu, X.F. Application of Combined Technology of Plain Concrete Diaphragm Wall Reinforcement and Closed Steel Sleeve in Shield Receiving. *Mod. Tunn. Technol.* **2020**, *57*, 980–984.
37. Wu, Q. Key Technology of Short Sleeve Shield Reception in Water-rich Gravel Stratum. *Urban Rapid Rail Transit* **2017**, *30*, 40–43+49.
38. He, W.G. Receiving Technology of Steel Sleeve for Shield Machine Under the Conditions of Local Block Ground. *Constr. Technol.* **2015**, *44*, 109–112.
39. Zhou, Y.K. Mechanical Deformation Characteristics and Soil Disturbance Analysis of the Launching Steel Sleeve of EPB Shield. Ph.D. Thesis, Beijing Jiaotong University, Beijing, China, 2018.

**Disclaimer/Publisher's Note:** The statements, opinions and data contained in all publications are solely those of the individual author(s) and contributor(s) and not of MDPI and/or the editor(s). MDPI and/or the editor(s) disclaim responsibility for any injury to people or property resulting from any ideas, methods, instructions or products referred to in the content.